5-2004

Microwave Radiation Force and Torque on a Disk Resonator Excited by a Circularly Polarized Plane Wave

Sergey N. Makarov
Worcester Polytechnic Institute, makarov@wpi.edu

S. Kulkarni

Microwave radiation force and torque on a disk resonator excited by a circularly polarized plane wave

S. Makarov[a] and S. Kulkarni
Department of Electrical and Computer Engineering, Worcester Polytechnic Institute, 100 Institute Road, Worcester, Massachusetts 01609-2280

(Received 27 January 2004; accepted 17 March 2004; published online 29 April 2004)

A numerical simulation method [S. Makarov and S. Kulkarni, Appl. Phys. Lett. **84**, 1600 (2004)] is used in order to determine the radiation force and radiation torque on a parallel-plate disk resonator, whose size is comparable to wavelength. The method is based on the MOM solution of the electric-field integral equation, accurate calculation of the near field, and removal of the self-interaction terms responsible for the pinch effect. The local force/torque distribution at the normal incidence of a circularly polarized plane wave is found. It is observed that, at the resonance, the individual disks are subject to unexpectedly large local force densities, despite the fact that the net radiation force on the resonator remains very small. On the other hand, the total axial torque on the disk resonator also increases at the resonance. © *2004 American Institute of Physics.*
[DOI: 10.1063/1.1739517]

The radiation forces and torques of a laser beam on small transparent dielectric objects were investigated long ago, both theoretically[1] and experimentally.[2,3] Recent (macro) applications of the optical radiation force include laser or optical tweezers (cf. Refs. 4 and 5) and optically driven microelectromechanical systems (Refs. 6 and 7). The advantage of applying the laser beam to a dielectric is the relatively high intensity of the primary field as well as a relatively low absorption loss in the transparent dielectric.

The radiation forces on metal targets received little attention. One portion of the work was devoted to very small metal particles.[8] On the other hand, one should perhaps mention limited research related to solar radiation pressure on satellites.[9,10] In that research, the radiation pressure is usually estimated using the basic high-frequency formula $p=(1+r)J/c$,[11] where J is the field intensity, c is the speed of light, and r is the reflection coefficient.

The finite metal targets are not very well suited for applying the laser beams, primarily due to large absorption. However, they may experience very significant *local* radiation force effects at rf and microwave frequencies, when the target is a resonator.[12] The present letter will investigate the radiation force and torque on a parallel-plate disk resonator, at the normal incidence of a circularly polarized (CP) plane wave. In this case, one may expect not only the high local radiation force but also a significant total axial torque.

The investigation is based on numerical simulation. A full-wave simulation using a three-dimensional version of the MoM solver for electric-field integral equation (EFIE) is employed. The scattered near field is accurately calculated in the vicinity of the surface grid.

The MoM formulation (metal scatterer) is rather standard and utilizes the mixed-potential approach to EFIE and the RWG basis functions.[13,14] We use the symmetric impedance matrix, which allows for a faster speed and larger memory storage. The double surface integrals are calculated using the Gaussian formulas of the fifth degree of accuracy.[15] All singular portions of self-integrals are found analytically, using the closed-form solutions given in Ref. 16. Factorization of the symmetric impedance matrix is done using the double precision simple driver ZSYSV of the LAPACK library[17] for symmetric complex matrixes.

The total Lorentz force density on the surface current and charge distribution on a metal surface is given by (cf., for example, Ref. 18)

$$\mathbf{f}=\tfrac{1}{2}\mathrm{Re}(\mathbf{J}_S\times\mathbf{B}^*)+\tfrac{1}{2}\mathrm{Re}(\sigma_S\mathbf{E}^*),\quad \mathbf{B}=\mu_0\mathbf{H}, \tag{1}$$

where $\mathbf{E}=\mathbf{E}^s+\mathbf{E}^i$, $\mathbf{H}=\mathbf{H}^s+\mathbf{H}^i$, and index i denotes the incident field. The scattered field $\mathbf{E}^s,\mathbf{H}^s$ are found numerically using already known current and charge densities $\mathbf{J}_S$ and σ_S—solutions of the MOM equations. The total Lorentz force $\mathbf{F}$ on a (open) metal surface S and the total radiation torque $\mathbf{M}$ are given by

$$\mathbf{F}=\int_S \mathbf{f}(\mathbf{r})ds,\quad \mathbf{M}=\int_S \mathbf{r}\times\mathbf{f}(\mathbf{r})ds. \tag{2}$$

For any small triangular patch on the metal surface, Eq. (2) contains a self-term that describes the interaction of the patch current and charge with the self-induced magnetic and electric fields. This effect cannot be described in terms of the model of an infinitesimally thin metal sheet (EFIE). The self-induced magnetic and electric fields are discontinuous on the sheet boundary so that Eq. (2) becomes meaningless. It is however well known that the interaction with the self-induced magnetic field in a volume conductor creates the pinch effect, where the metal sheet is squeezed in the transversal direction but does not experience any net force. The pinch force is thus of no interest for the present problem. The charge interaction with the self-induced electric field (being normal to the surface) might also give a contribution to the pinch force. Thus, the following assumption is made with finding the force in Eq. (2). For any small triangular patch on the metal surface, Eq. (2) will ignore its own contribution to the fields $\mathbf{E}^s,\mathbf{H}^s$ but take into account contributions of all other patches. In other words, the patch currents and charges

[a]Electronic mail: makarov@wpi.edu

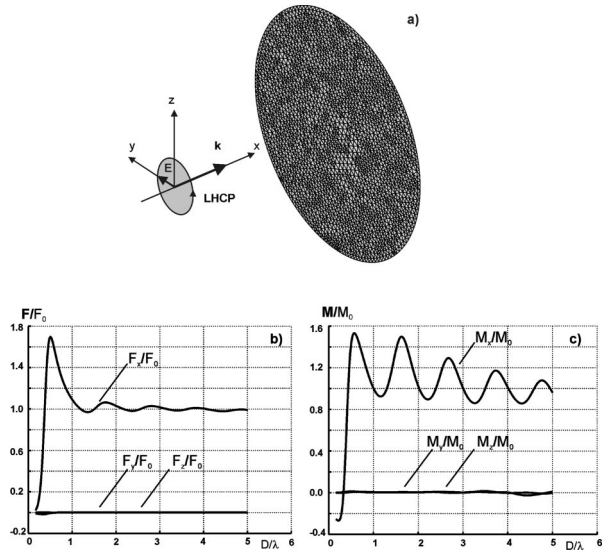

FIG. 1. (a) Geometry of the incident signal for a single disk and (b), (c) net radiation force and torque as a function of the ratio diameter/wavelength. The original (simulation) disk mesh has 4657 triangles (6913 unknowns); 250 frequency steps are employed to cover the entire domain of D/λ.

will interact with the fields of all other patches but will not interact with their own fields. This assumption seems to become more accurate for finer surface triangular meshes and was extensively tested.

The net radiation force on a single disk at normal incidence of a left-handed CP wave [Fig. 1(a)] is found in Fig. 1(b). The disk mesh shown on Fig. 1(a) has 4657 triangles (6913 unknowns), which allows us to cover higher frequencies with up to four to five wavelengths along the disk diameter $D=2R$. Figure 1(b) shows three components of the total

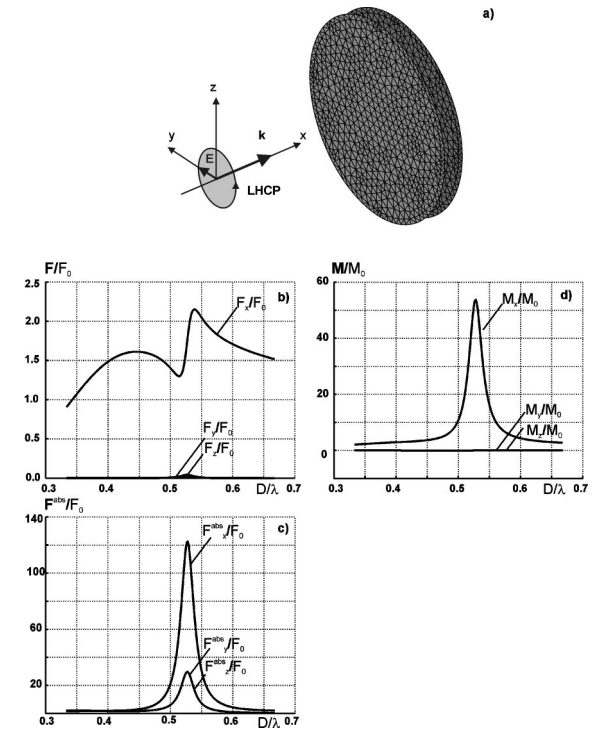

FIG. 2. (a) Geometry of the incident signal for the air-filled parallel-plate disk resonator, (b) net radiation force as a function of the ratio diameter/wavelength, (c) magnitude of the force density integrated over the surface area, and (d) net radiation torque on the resonator.

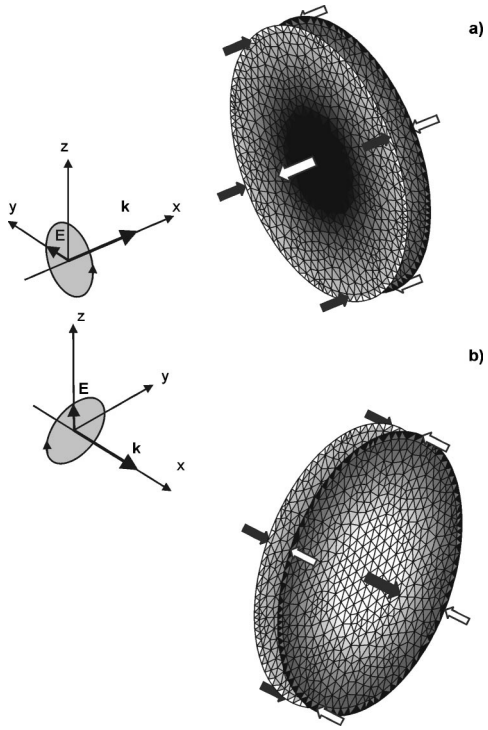

FIG. 3. (a) Force density distribution for the parallel-plate disk resonator with $d/R=0.2$ at the fundamental resonance—illuminated zone. The surface gray scale extends from black (maximum force density in the direction of the negative x axis) to white (maximum force density in the direction of the positive x axis) and (b) the same results for the shadow zone. A very similar (with regard to force direction) distribution takes place in the case of a right-handed CP signal.

radiation force $\mathbf{F}$ on the disk as functions of the ratio D/λ. The resulting total torque on the disk is shown in Fig. 1(c). The total force is normalized to its high-frequency limit $F_0=2\times\pi R^2\ J/c$, where J is the intensity of the incident signal. The total torque is normalized to $M_0=-2\times\pi R^3\ J/c$, in order to have a positive angular component.

One can see that the axial force F_x asymptotically tends to F_0 at higher frequencies. At lower frequencies and, especially close to the first resonance, the force values appear to be somewhat higher than the high-frequency limit. The components F_y, F_z are insignificant due to symmetry reasons. Also, the magnetic (Lorentz) component of the force in Eq. (1) clearly dominates as it follows from the solution analysis. One can also see that the dominant torque component is directed along the positive x axis (after normalization), as suggested by the transport of angular momentum by the CP wave.[19] Two other torque components are negligibly small due to symmetry.

The scattering analysis of plate resonators has been among the first to be carried out by computers about 40 years ago.[20] Eigenmode charts are available for basic resonator shapes.[21,22] However, the data on the radiation force or torque was not yet reported.

The net radiation force on a parallel-plate disk resonator [Fig. 2(a)] is found in Fig. 2(b). The resonant frequency approximates that of the TM^x_{110} mode ($k_{11}\approx 1.8$),[22] where first two indices indicate the angular and radial numbers of zeros of the Bessel functions. The distance, d, between disks is $R/5$. The behavior of the net force is relatively smooth close to the resonance. The opposite situation however occurs if

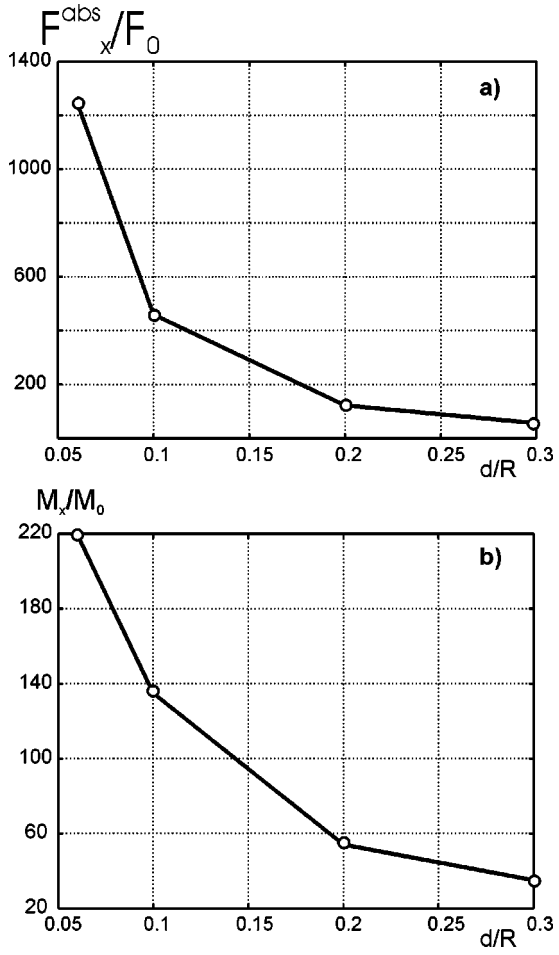

FIG. 4. (a) Magnitude of the force density integrated over the surface area, F_x^{abs}, for resonators with different ratios d/R (quality factor) at the fundamental resonance and (b) total axial torque for different ratios d/R at the fundamental resonance.

we consider the absolute value (magnitude) of the force density and then integrate the result over the surface area. Figure 2(c) shows the result for

$$F_{x,y,z}^{\mathrm{abs}} = \int_S |f_{x,y,z}(\mathbf{r})| ds. \tag{3}$$

One can see that F_x^{abs} at the resonance is nearly 120 times the high-frequency limit F_0. The absolute force on a single disk is approximately one half of this value.

To understand why F_x^{abs} is so different from the net force, we plotted the local force distribution. In Fig. 3, the surface shading indicates the surface values of the local force density, $f_x(\mathbf{r})$, for the same resonator. The white color in Fig. 3 corresponds to positively directed force density (along the x axis) whereas the black color indicates the opposite direction. The local force density becomes very high at the resonance. However, integrally, the forces cancel each other. This cancellation takes place not only between two disks but also for every individual disk. It is found that this is the contribution of the electric component of the force (insignificant for the single disk) that is responsible for such a cancellation. On the other hand, the net angular momentum [Fig. 2(d)] increases at the resonance and reaches about 54 times its value for the single disk.

Similar results were observed for several other resonators that use the following d/R ratios: $d/R=0.3$, 0.2, 0.1, and 0.06. The corresponding Q factor of the resonator is calculated as $Q=14$, 21, 39, and 65. The corresponding eigenfrequency at $D=0.1$ m is calculated as $f_{\mathrm{res}} \approx 1.52$, 1.58, 1.65, and 1.69 GHz. Figure 4(a) shows the maximum of F_x^{abs} at the resonance as a function of disk spacing. One can see that F_x^{abs} may be as high as $1200F_0$ at $Q=65$ and tends to increase when the distance between plates decreases (Q of the resonator increases). The absolute force for a single plate is approximately $0.5F_x^{\mathrm{abs}}$. A similar behavior is observed for the net axial torque [Fig. 4(b)].

We have shown that the F_x^{abs} may be as high as 1200 times its high-frequency limit for the parallel-plate disk resonator at the normal incidence of the CP plane wave. The total axial torque on the resonator with $Q=65$ appears approximately 200 times higher than the torque on a single disk of the same size. While the result for torque may be explained by increasing the scattering cross section at the resonance, the result for the local force distribution probably requires a different explanation.

[1] J. P. Barton, D. R. Alexander, and S. A. Schaub, J. Appl. Phys. **66**, 4594 (1989).
[2] A. Ashkin, Phys. Rev. Lett. **24**, 156 (1970).
[3] A. Ashkin, IEEE J. Sel. Top. Quantum Electron. **6**, 841 (2000).
[4] Y. Nahmias and D. J. Odde, IEEE J. Quantum Electron. **38**, 131 (2002).
[5] A. B. Nemet, Y. Shabtai, and M. Cronin-Golomb, Opt. Lett. **27**, 264 (2002).
[6] W. L. Collett, C. A. Ventrice, and S. M. Mahajan, Appl. Phys. Lett. **82**, 2730 (2003).
[7] E. Higurashi, O. Ohguchi, T. Tamamura, and H. Ukita, J. Appl. Phys. **82**, 2773 (1997).
[8] K. Svoboda and S. M. Block, Opt. Lett. **19**, 930 (1994).
[9] S. N. Singh, IEEE Trans. Aerosp. Electron. Syst. **32**, 732 (1996).
[10] R. Venkatachalam, IEEE Trans. Aerosp. Electron. Syst. **29**, 1164 (1993).
[11] P. N. Lebedev, Annalen der Physik **6**, 433 (1901).
[12] S. Makarov and S. Kulkarni, Appl. Phys. Lett. **84**, 1600 (2004).
[13] A. F. Peterson, S. L. Ray, and R. Mittra, *Computational Methods for Electromagnetics* (IEEE, Piscataway, New Jersey, 1998).
[14] S. M. Rao, D. R. Wilton, and A. W. Glisson, IEEE Trans. Antennas Propag. **30**, 409 (1982).
[15] G. R. Cowper, Int. J. Numer. Methods Eng. , 405 (1973).
[16] T. F. Eibert and V. Hansen, IEEE Trans. Antennas Propag. **43**, 1499 (1995).
[17] E. Anderson, Z. Bai, C. Bischof, S. Blackford, J. Demmel, J. Dongarra, J. Du Croz, A. Greenbaum, S. Hammarling, A. McKenney, and D. Sorensen, "LAPACK User's Guide," 3rd ed. (SIAM, 1999).
[18] D. Yaghjian, Antennas and Propagation Society, 2001 IEEE International Sym. **4**, 2868 (1999).
[19] P. L. Marston and J. H. Crighton, Phys. Rev. A **30**, 2508 (1984).
[20] A. G. Fox and T. Li, Bell Syst. Tech. J. **40**, 458 (1961).
[21] K. Adam, D. A. Kaklamani, and N. K. Uzonoglu, Antennas and Propagation Society, 1997 IEEE International Sym. **1**, 302 (1999).
[22] A. Eriksson, P. Linnér, and S. Gevorgian, IEE Proc. - Microw. Antennas Propag. **148**, 51 (2001).